

Photorelaxation Induced by Water–Chromophore Electron Transfer

Mario Barbatti*

Max-Planck-Institut für Kohlenforschung, Kaiser-Wilhelm-Platz 1, D-45470 Mülheim an der Ruhr, Germany

S Supporting Information

ABSTRACT: Relaxation of photoexcited chromophores is a key factor determining diverse molecular properties, from luminescence to photostability. Radiationless relaxation usually occurs through state intersections caused by distortions in the nuclear geometry of the chromophore. Using excited-state nonadiabatic dynamics simulations based on algebraic diagrammatic construction, it is shown that this is the case of 9H-adenine in water cluster, but not of 7H-adenine in water cluster. 7H-adenine in water cluster relaxes via a state intersection induced by electron transfer from water to the chromophore. This result reveals an unknown reaction pathway, with implications for the assignment of relaxation mechanisms of exciton relaxation in organic electronics. The observation of photorelaxation of 7H-adenine induced by water–chromophore electron transfer is a proof of principle calling for further computational and experimental investigations to determine how common this effect is.

In the last two decades, it became clear that state crossings play a central role for internal conversion.^{1,2} When involving the ground and the first excited states, such crossings are usually caused by strong distortions of the molecular geometry, such as bond dissociation,³ bond twist,⁴ or ring puckering.⁵ Most of time, the environment is assumed to play an important but passive role: it helps to tune the specific topography of the reaction pathways, shifting the energies of stationary states and state crossings up and down; however, the environment is not expected to directly contribute to the state crossing itself. During my investigations of the relaxation of two tautomers of photoexcited adenine in water clusters, I found out that 9H-adenine in water cluster exemplary corresponds to such conventional description. Its relaxation process is very similar to what is observed in the gas phase.^{6,7} Nevertheless, the relaxation of 7H-adenine in water cluster was deeply distinct from that in the gas phase, with the electronic structure of one of the water molecules actively contributing to the formation of the state crossing where internal conversion to the ground state took place. This finding comes to join another previously identified solvent–chromophore excited-state pathway, the proton-coupled electron transfer described in refs 8 and 9.

The initial motivation to investigate the nonadiabatic dynamics of UV-excited adenine tautomers is that the understanding of how nucleic acid fragments, from nucleobases to double-strands, react to photoexcitations is a key step to comprehend mutagenesis, carcinogenesis,^{10,11} and the development of life in early biotic era.^{12,13} During the last years, experimental and theoretical works have unveiled how different

types of phenomena—internal conversion,^{5,14} exciton delocalization,^{15,16} intersystem crossing¹⁷—are involved in nucleic acid photorelaxation. These works have also showed how many variables like tautomeric effects, fragment nature (isolated bases, base pairs, stacked bases), and solvation state play different roles to determine the main reaction pathways that are followed after photoexcitation.¹⁸ In spite of the importance of this biomolecular framework on itself, the findings of the present simulations are more general, with potential implications for diverse fields of research.

Time-resolved spectroscopy of adenine in the gas phase shows a single time constant of 1.2 ps after excitation at 267 nm.^{19,20} In water, adenine shows two time constants, 0.18 ± 0.03 and 8.8 ± 1.2 ps (263 nm).²¹ Either in gas or in water, these short excited-state deactivation times are undisputed evidence that UV-excited adenine relaxes back to the ground state via internal conversion. In the case of adenine in water, the two time constants have been assigned to the two main tautomers of adenine, the short to 9H-adenine and the long to 7H-adenine.^{21–24} Although it is not clear why these tautomers would relax with different time constants (see refs 25 and 26 for their reaction paths in the gas phase), the validity of this assignment has been taken for granted, as it leads to estimate of tautomeric populations consistent with other measurements.²¹

So far, it has been challenging to use dynamics simulation methods to determine the relaxation mechanism of solvated adenine due to, on one hand, the large size of quantum-mechanical active site consisting of adenine plus the first shell of waters and, on the other hand, the failure of the time-dependent density functional theory to describe this system.²⁷ Recent developments in the field, including the possibility of performing nonadiabatic dynamics⁷ with algebraic diagrammatic construction to the second order [ADC(2)]^{28,29} has made possible to simulate how different solvated tautomers react to UV excitation.

My working hypothesis is that the main impact of the solvation on the excited-state evolution is due to the few water molecules directly hydrogen bonded to adenine. Thus, I ran excited-state nonadiabatic dynamics simulations of 7H- and 9H-adenine within small water clusters using the surface hopping method, based on ADC(2) potential energy surfaces and couplings.

The optimized clusters for both tautomers are shown in Figure 1a,b (see Supporting Information, SI, for details on geometries and excitation spectra). For 9H-adenine, the minimal cluster has six waters, while for 7H-adenine, it has five waters. Starting from the ground-state optimized clusters,

Received: May 29, 2014

Published: July 10, 2014

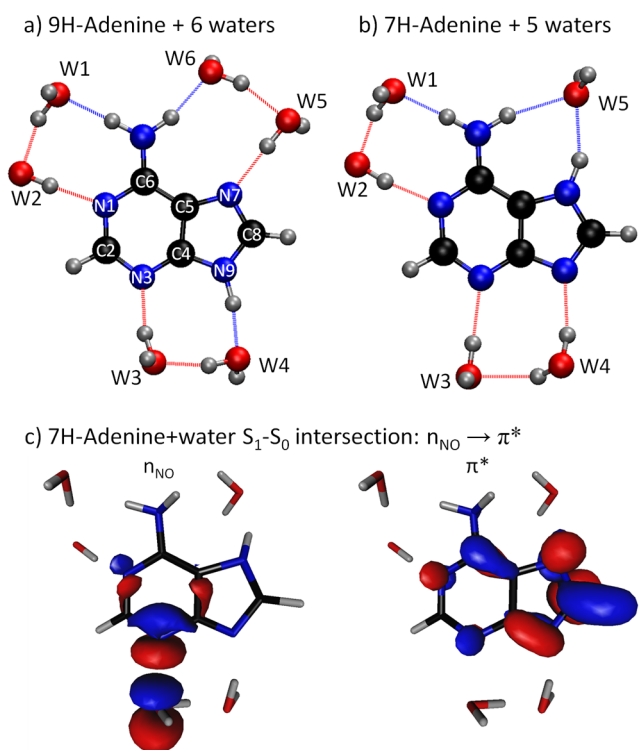


Figure 1. Ground-state structure of (a) 9H-adenine + water and (b) 7H-adenine + water. (c) Singly-occupied orbitals at the electron-transfer state intersection for 7H-adenine + water.

the absorption spectra were computed. Spectral points in the 4.71 ± 0.05 eV (~ 263 nm, Figure 2) domain were taken to start the dynamics.

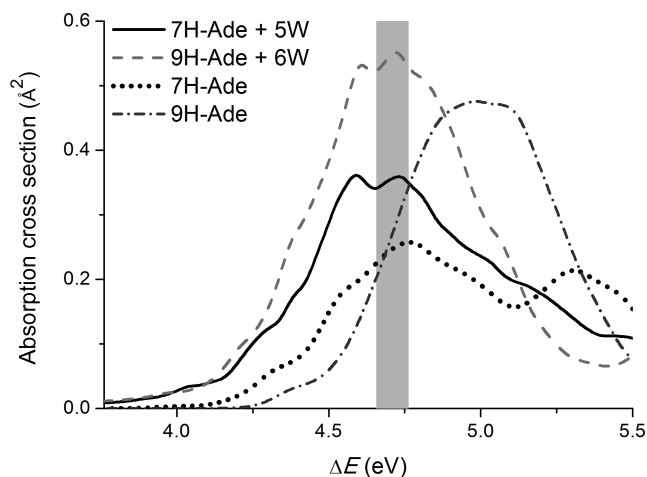


Figure 2. Simulated absorption spectrum of adenine tautomers in water clusters and in the gas phase. Initial conditions for dynamics were sampled from the shaded area.

The results of the simulations show that, in fact, the relaxation of 9H-adenine in water cluster should contribute only to the short time constant. The distribution of relaxation times can be fitted with a single decay function (see SI), giving a time constant of 0.22 ps (Table 1). Most of trajectories (90%) followed a pathway ending at a state intersection caused by a strong out-of-plane distortion of C2 (C2 puckering), very similar to what is observed in the gas phase.⁷ Few trajectories

Table 1. Excited-State Lifetime τ and Fraction of the Population f_0 Not Deactivated within the Ultrafast Step for Adenine Tautomers in the Gas Phase (GP) and in Water (W) Clusters

		f_0	τ (ps)	
			theor.	expt.
7H-Ade	GP	0.00	1.47	1.2 ^a
9H-Ade	GP	0.00	1.12	
7H-Ade	W	0.31	0.37, >1	0.18, 8.8 ^b
9H-Ade	W	0.00	0.22	

^aPump: 267 nm.^{19,20} ^bPump: 263 nm.²¹ (Experimental Data for All Tautomers Together)

relaxed at C6-puckered intersections (4%) or at adenine-water proton-transfer intersections (6%). (See SI for statistical errors.)

In the case of 7H-adenine in water cluster, differently from the experimental assignment, the simulations showed that this tautomer should contribute not only to the long but also to the short time constant. The fitting of the relaxation time distribution shows that 69% of 7H-adenine population relaxes with a time constant of 0.37 ps, while the remaining 31% relaxes with a time constant that is much longer than 1 ps, the maximum simulation time (Table 1).

Even more surprising is that ring-puckered intersections only accounted for a minor fraction of the relaxation processes in 7H-adenine (12% of trajectories). Most of trajectories (58%) followed a completely new relaxation pathway ending at a S_1/S_0 intersection where 7H-adenine is almost planar. At this planar intersection, the S_1 state consists of an electron excitation from lone-pair orbitals at N3 and at the nearest oxygen into a π^* orbital at the imidazole ring. The main mechanistic feature inducing the intersection is a rotation of the water near N3 (W3 in Figure 1b), which goes from an OH \cdots N3 conformation in the ground-state geometry to a conformation with oxygen lone pair facing the N3 lone pair (Figures 1c and 3; see also the movies in the SI). A natural population analysis of the S_1

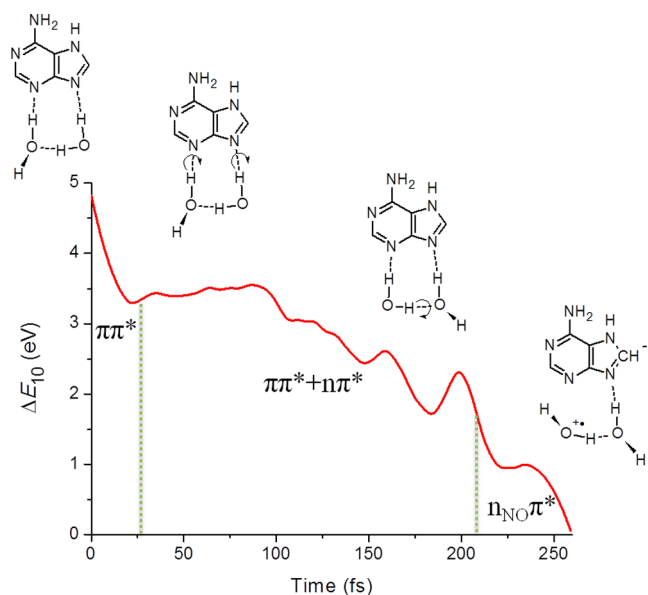


Figure 3. Energy-gap evolution in a representative trajectory of 7H-adenine in water.

density at this intersection geometry shows that W3 transfers 0.4 electron to the imidazole group. In fact, the statistical analysis of the S_1 charge transfer at the intersection point for all trajectories resulted in a mean value of 0.4 ± 0.1 electron transferred from water to 7H-adenine.

The geometry of the S_1 – S_0 intersection is shown in Figure 4 (see SI). It is the lowest-energy intersection occurring during

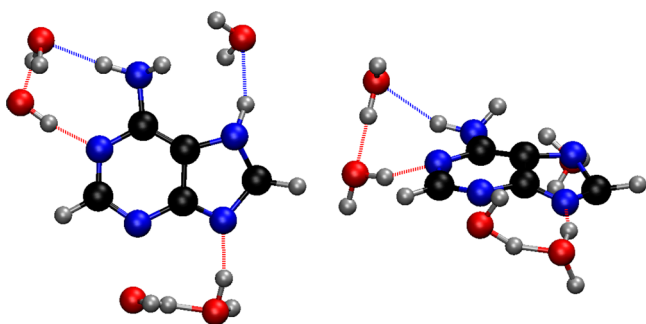


Figure 4. Top and lateral views of the S_1 – S_0 intersection in 7H-adenine in water.

the dynamics. The S_1 – S_0 energy gap is 0.11 eV. Conical-intersection optimization³⁰ starting from this structure does not change it significantly. Although the rings are essentially planar, N7 and C8 are slightly pyramidalized to accommodate the excess of electron charge in the imidazole ring.

Other local minima may be accessible at similar energies for such clusters and also bulk effects may play a role in the final quantitative results. For this work, however, only the occurrence of relaxation induced by water–chromophore electron transfer matters. It is a proof that in principle this effect may take place after photoexcitation of solvated chromophores. Besides that, the modeling of clusters, initially aimed at simplifying the problem, should be seen under new light. In the future, the search for experimental evidence of this new path may profit of cleaner spectra measured for small clusters³¹ as compared to those measured in bulky water.

Proton transfer after the electron transfer was not observed. This implies that either it is classically forbidden or there is not enough time for its occurrence before the internal conversion takes place. Tunneling is not considered in the modeling, but, again, the time between the population of the electron-transfer state and the internal conversion (~ 50 fs) may be too short for its occurrence.

Dynamics of both tautomers in the gas phase was also simulated. 9H-adenine relaxation splits between C2- and C6-puckered pathways, as reported before.⁷ The lifetime is 1.12 ps (Table 1). 7H-adenine relaxes preferentially through C6-puckered intersections, with 1.47 ps lifetime. Assuming a tautomeric population of 20% of 7H and 80% of 9H,²¹ the lifetime is 1.2 ps, in excellent agreement with the experimental time constant (1.2 ps for 267 nm excitation).^{19,20}

As mentioned above, state intersections between the ground and the first excited states are normally associated with strong distortions of the nuclear frame. These distortions are needed because to have a state crossing, it is necessary to simultaneously stabilize the energy of the excited state and destabilize the ground state. This is what happens, for instance, during ring puckering. In the planar intersection, however, the crossing was produced not by distortion of the excited chromophore geometry, but by rearrangement of the solvation

shell followed by population of a electron-transfer state. (State and geometry evolutions are discussed in the SI.) This process opens the possibility of having internal conversion even in situations where steric interactions tend to hinder the chromophore distortion.

The active role of water to create state intersections has eluded experimentalists and theorists so far due to a few different reasons. First, it may not be a widespread effect. As we have seen, 9H-adenine is not affected by this effect, and at this point it is admittedly too soon to know how common it is. Second, time constants for internal conversion in different environments are usually similar, which induces us to believe that the same qualitative process is taking place. In fact, this expectation has affected previous simulations in the field, which commonly took water into account either as a continuum or as a molecular force field.^{32,33} (Neither of these approaches can describe changes in the electronic structure of the solvent, only its perturbation to the environment.) Even simulations considering explicit quantum-mechanical solvent also missed the effect either for dealing only with the 9H tautomer or for focusing on traditional reaction paths.^{34,35} Thus, the manifestation of this water–chromophore electron-transfer intersection had to wait for simulations combining dynamics, different tautomers, and explicit quantum-mechanical solvation. (For a recent discussion of the excited states of water clusters see ref 36.)

These results have also two important consequences. First, it reinforces the idea that the solvent–chromophore electron-transfer pathways need to be considered in the assignment of relaxation mechanisms chromophores in polar solvents.⁹ Second, the possibility that the environment may create state intersections upon photoexcitation may have relevant implications for organic electronics, where internal conversion to the ground state is often a factor reducing the efficiency of photovoltaic devices.³⁷

Here I showed that photorelaxation induced by water–chromophore electron transfer is a major internal conversion pathway for one specific tautomer of adenine. This new phenomenon is interesting enough to be already communicated to the chemistry community. Nevertheless, there is still a long way to go from this proof of principle to a more robust characterization. There are a number of questions to be addressed by computational simulations, including the reason why this pathway is not activated in 9H-adenine, whether it happens with other polar solvents, and how it is affected by the water bulk. Naturally, it also rests the challenge of characterizing this effect experimentally, which may possibly be achieved by time-resolved photoelectron spectroscopy of selected tautomers within small water clusters.

Computational Methods. Ab-initio algebraic diagrammatic construction to the second order [ADC(2)]²⁸ was used to simulate the nonadiabatic dynamics of 9H and 7H tautomers of adenine in small water clusters. Clusters were optimized in the ground state with the Møller–Plesset perturbation theory to the second order (MP2; Cartesian coordinates are given in the SI). aug-cc-pVDZ and cc-pVDZ basis sets were assigned to N and C atoms, respectively.³⁸ SVP basis set³⁹ was assigned to O and H atoms. The nuclear ensemble method⁴⁰ with 500 points and 5 excited states was used to simulate the absorption spectrum, from where initial conditions for dynamics were selected. 50 trajectories for each tautomer with water and in the gas phase were started from the 4.71 ± 0.05 eV (~ 263 nm) spectral window, summing to a total of 200 trajectories. For

7H-adenine in water, this window corresponded to 47 trajectories starting in S_1 and 3 trajectories in S_2 . For 7H-adenine in the gas phase, this distribution was 25 and 25. For 9H-adenine in water, 41 and 9. For 9H-adenine in the gas phase, 33 and 17. Nonadiabatic effects between excited states were taken into account via fewest-switches surface hopping⁴¹ with decoherence corrections.⁴² With ADC(2), only non-adiabatic transitions between excited states can be computed.⁷ Thus, for each trajectory, the time for internal conversion to the ground state was estimated by the first time in which the energy gap between the first excited state and the ground state dropped below 0.15 eV. Trajectories were integrated until this threshold was reached or for a maximum of 1 ps. The time step for integration of classical equations was 0.5 fs and of quantum equations, 0.025 fs. All calculations were done with Turbomole⁴³ and Newton-X^{44,45} programs. Detailed information about the methods and approximations is provided in the SI.

■ ASSOCIATED CONTENT

■ Supporting Information

Movies with trajectory examples. Computational details. Geometries, vertical excitations, and spectra. Statistical analysis of simulations. Analysis of a single trajectory. Comparison to fully correlated data. Dipole moments and ionization potentials at the intersections. Cartesian coordinates. This material is available free of charge via the Internet at <http://pubs.acs.org>.

■ AUTHOR INFORMATION

Corresponding Author

barbatti@kofo.mpg.de

Notes

The author declares no competing financial interest.

■ ACKNOWLEDGMENTS

The author acknowledges generous computer time provided by the Max-Planck-Institut für Kohlenforschung.

■ REFERENCES

- (1) Domcke, W.; Yarkony, D. R.; Köppel, H. *Conical Intersections - Theory, Computation and Experiment*; World Scientific: Singapore, 2011.
- (2) Domcke, W.; Yarkony, D. R.; Köppel, H. *Conical Intersections - Electronic Structure, Dynamics and Spectroscopy*; World Scientific: Singapore, 2004.
- (3) Schultz, T.; Samoylova, E.; Radloff, W.; Hertel, I. V.; Sobolewski, A. L.; Domcke, W. *Science* **2004**, *306*, 1765–1768.
- (4) Polli, D.; Altoe, P.; Weingart, O.; Spillane, K. M.; Manzoni, C.; Brida, D.; Tomasello, G.; Orlandi, G.; Kukura, P.; Mathies, R. A.; Garavelli, M.; Cerullo, G. *Nature* **2010**, *467*, 440–443.
- (5) Barbatti, M.; Aquino, A. J. A.; Szymczak, J. J.; Nachtigallová, D.; Hobza, P.; Lischka, H. *Proc. Natl. Acad. Sci. U.S.A.* **2010**, *107*, 21453–21458.
- (6) Conti, I.; Garavelli, M.; Orlandi, G. *J. Am. Chem. Soc.* **2009**, *131*, 16108–16118.
- (7) Plasser, F.; Crespo-Otero, R.; Pederzoli, M.; Pittner, J.; Lischka, H.; Barbatti, M. *J. Chem. Theory Comput.* **2014**, *10*, 1395–1405.
- (8) Sobolewski, A. L.; Domcke, W. G. *J. Phys. Chem. A* **2007**, *111*, 11725–11735.
- (9) Liu, X.; Sobolewski, A. L.; Borrelli, R.; Domcke, W. *Phys. Chem. Chem. Phys.* **2013**, *15*, 5957–5966.
- (10) Douki, T. *Photochem. Photobiol. Sci.* **2013**, *12*, 1286–1302.
- (11) Crespo-Hernández, C. E.; Cohen, B.; Kohler, B. *Nature* **2005**, *436*, 1141–1144.
- (12) Sandford, S. A.; Bera, P. P.; Lee, T. J.; Materese, C. K.; Nuevo, M. *Top. Curr. Chem.* **2014**, DOI: 10.1007/1128_2013_1499.
- (13) Boulanger, E.; Anoop, A.; Nachtigallová, D.; Thiel, W.; Barbatti, M. *Angew. Chem., Int. Ed.* **2013**, *52*, 8000–8003.
- (14) Canuel, C.; Mons, M.; Piuze, F.; Tardivel, B.; Dimicoli, I.; Elhanine, M. *J. Chem. Phys.* **2005**, *122*, 074316–074316.
- (15) Banyasz, A.; Gustavsson, T.; Onidas, D.; Changenet-Barret, P.; Markovitsi, D.; Improta, R. *Chem.—Eur. J.* **2013**, *19*, 3762–3774.
- (16) Takaya, T.; Su, C.; de La Harpe, K.; Crespo-Hernández, C. E.; Kohler, B. *Proc. Natl. Acad. Sci. U.S.A.* **2008**, *105*, 10285–10290.
- (17) Mai, S.; Marquetand, P.; Richter, M.; González-Vázquez, J.; González, L. *ChemPhysChem* **2013**, *14*, 2920–2931.
- (18) Middleton, C. T.; de La Harpe, K.; Su, C.; Law, Y. K.; Crespo-Hernández, C. E.; Kohler, B. *Annu. Rev. Phys. Chem.* **2009**, *60*, 217–239.
- (19) Satzger, H.; Townsend, D.; Zgierski, M. Z.; Patchkovskii, S.; Ullrich, S.; Stolow, A. *Proc. Natl. Acad. Sci. U.S.A.* **2006**, *103*, 10196–10201.
- (20) Satzger, H.; Townsend, D.; Stolow, A. *Chem. Phys. Lett.* **2006**, *430*, 144–148.
- (21) Cohen, B.; Hare, P. M.; Kohler, B. *J. Am. Chem. Soc.* **2003**, *125*, 13594–13601.
- (22) Buchner, F.; Ritzke, H.-H.; Lahl, J.; Lubcke, A. *Phys. Chem. Chem. Phys.* **2013**, *15*, 11402–11408.
- (23) Pancur, T.; Schwalb, N. K.; Renth, F.; Temps, F. *Chem. Phys.* **2005**, *313*, 199–212.
- (24) Gustavsson, T.; Sharonov, A.; Onidas, D.; Markovitsi, D. *Chem. Phys. Lett.* **2002**, *356*, 49–54.
- (25) Marian, C. M.; Kleinschmidt, M.; Tatchen, J. *Chem. Phys.* **2008**, *347*, 346–359.
- (26) Serrano-Andrés, L.; Merchán, M.; Borin, A. C. *Chem.—Eur. J.* **2006**, *12*, 6559–6571.
- (27) Barbatti, M.; Lan, Z.; Crespo-Otero, R.; Szymczak, J. J.; Lischka, H.; Thiel, W. *J. Chem. Phys.* **2012**, *137*, 22A503–514.
- (28) Hättig, C. *Adv. Quantum Chem.* **2005**, *50*, 37–60.
- (29) Schirmer, J. *Phys. Rev. A* **1982**, *26*, 2395–2416.
- (30) Levine, B. G.; Coe, J. D.; Martínez, T. J. *J. Phys. Chem. B* **2008**, *112*, 405–413.
- (31) Kim, N. J.; Kang, H.; Jeong, G.; Kim, Y. S.; Lee, K. T.; Kim, S. K. *J. Phys. Chem. A* **2000**, *104*, 6552–6557.
- (32) Conti, I.; Altoe, P.; Stenta, M.; Garavelli, M.; Orlandi, G. *Phys. Chem. Chem. Phys.* **2010**, *12*, 5016–5023.
- (33) Lan, Z.; Lu, Y.; Fabiano, E.; Thiel, W. *ChemPhysChem* **2011**, *12*, 1989–1998.
- (34) Gustavsson, T.; Sarkar, N.; Vaya, I.; Jimenez, M. C.; Markovitsi, D.; Improta, R. *Photochem. Photobiol. Sci.* **2013**, *12*, 1375–1386.
- (35) Mitrić, R.; Werner, U.; Wohlgenuth, M.; Seifert, G.; Bonačić-Koutecký, V. *J. Phys. Chem. A* **2009**, *113*, 12700–12705.
- (36) Segarra-Martí, J.; Coto, P. B.; Rubio, M.; Roca-Sanjuán, D.; Merchán, M. *Mol. Phys.* **2013**, *111*, 1308–1315.
- (37) Brédas, J.-L.; Norton, J. E.; Cornil, J.; Coropceanu, V. *Acc. Chem. Res.* **2009**, *42*, 1691–1699.
- (38) Dunning, T. H. *J. Chem. Phys.* **1989**, *90*, 1007–1023.
- (39) Weigend, F.; Ahlrichs, R. *Phys. Chem. Chem. Phys.* **2005**, *7*, 3297–3305.
- (40) Crespo-Otero, R.; Barbatti, M. *Theor. Chem. Acc.* **2012**, *131*, 1237.
- (41) Tully, J. C. *J. Chem. Phys.* **1990**, *93*, 1061–1071.
- (42) Granucci, G.; Persico, M. *J. Chem. Phys.* **2007**, *126*, 134114–134111.
- (43) Ahlrichs, R.; Bär, M.; Häser, M.; Horn, H.; Kölmel, C. *Chem. Phys. Lett.* **1989**, *162*, 165–169.
- (44) Barbatti, M.; Ruckebauer, M.; Plasser, F.; Pittner, J.; Granucci, G.; Persico, M.; Lischka, H. *WIREs: Comp. Mol. Sci.* **2014**, *4*, 26–33.
- (45) Barbatti, M.; Granucci, G.; Ruckebauer, M.; Plasser, F.; Crespo-Otero, R.; Pittner, J.; Persico, M.; Lischka, H. *NEWTON-X: a package for Newtonian dynamics close to the crossing seam*; Max-Planck-Institut für Kohlenforschung: Germany, 2013; www.newtonx.org.